Low-Temperature Chemical Solution Synthesis and Characterization of Nanocrystalline Fe-doped ZnO

A. Parra-Palomino, R. Singhal, O. Perales Perez*, S. Dussan-Devia and M. S. Tomar

University of Puerto Rico, Mayagüez, PR 00680-9044, Puerto Rico, *ojuan@uprm.edu.

ABSTRACT

The recent finding of multifunctional semiconductor materials with magnetic and optical properties has attracted scientific and technological attention due to their potential applications in nanotechnology and spintronics. We present here our results on synthesis and characterization of bare and Fe-doped ZnO nanocrystals by a modified sol-gel method, which does not require annealing of the samples. XRD characterization of the products confirmed the exclusive formation of the host ZnO wurtzite structure, with an average crystallite size between 11-13 nm. FT-IR analyses of the samples suggested the adsorption of acetate species, from precursor metal salts, onto the oxide surface. UV-Vis absorption data evidenced the decrease in the value of the band gap energy with increasing the atomic fraction 'x', of dopant Fe. This red shift is attributed to the *sp-d* exchange interaction between the band electrons and the localized d electrons of the Fe^{2+} substituting Zn ions. Raman measurements confirmed the Fe doping in ZnO.

Keywords: low-temperature synthesis, chemical solution synthesis, Fe-doped ZnO, nanoparticles.

1 INTRODUCTION

Recently, diluted magnetic semiconductors are of great interest due to its wide range of technological applications to optoelectronic [1], magnetoelectronic, microwave devices, laser diodes (LDs), surface acoustic wave (SAW) filter devices [2] and transparent thin film transistor [3], etc. Wurtzite-type ZnO and its compounds are found to be of great interest because of is wide band gap (3.29 eV) and large exciton binding energy (60meV). Several experimental works [4,5] have been carried out to synthesize ZnO nanoparticles under size-controlled conditions and study their optical behavior at the nanoscale. It has been reported by several researchers that the diluted magnetic semiconductors formed by replacing the cations of III-IV or II-VI nonmagnetic semiconductors by ferromagnetic Mn, Fe, Co species, exhibit unique magnetic, magneto-optical and magneto-transport properties, applicable for magneto-electronic and spintronics devices. It has already been theoretically predicted by several authors [6,7] that ferromagnetism above room temperature may be possible in 3d transition metal doped ZnO. It is also a good choice for the synthesis of transparent ferromagnetic material. Kim and Park [8], have prepared $Zn_{1-x}Co_xO$ ($x \leq 0.22$) films on Al_2O_3 substrate by rf magnetron sputtering. Thota and coworkers [9] have synthesized transition metal doped ZnO ($Zn_{1-x}M_xO$, $0 \leq x \leq 0.30$, M = Ni, Mn, Co) by a sol-gel route where the intermediate must be annealed at 500^0C for 2 hours to develop the oxide structure. They also found that doping on ZnO took place along with a variation in lattice parameter. They also verified that the incorporation of Ni and Co in ZnO was less than 10% and of manganese was between 10% and 15%. In the present work, we present the results on synthesis and structural, optical and magnetic characterization of Fe doped ZnO nanoparticles. Doped nanocrystals were synthesized through a chemical route with no need of thermal treatment to reveal the oxide structure.

2 EXPERIMENTAL

Zinc acetate dihydrate [$Zn(OOCCH_3)\cdot 2H_2O$, Aldrich, 99.99%] and iron acetate [$Fe(CO_2CH_3)_2$, Aldrich, 99.995%] were used as precursors for Zn and Fe, respectively. 2-ethylhexanoic acid [Alfa Aesar], with a boiling point of 250 ^{o}C, was used as solvent. Suitable amounts of iron and zinc acetate salts were dissolved for different Fe atomic fractions, 'x', in ZnO (x= 0.01-0.1), followed by continuous stirring and heating. The brown Fe-Zn solution was refluxed at about 200 ^{o}C for 15 minutes. Solvent was removed out by drying in air to obtain the powder. The formation of the oxide structures takes place just after the evaporation of the solvent, making any thermal treatment unnecessary. Powdered samples were ground using an agate mortar and submitted for characterization.

2.1 Characterization Techniques

The crystal structure and crystalline quality of Fe-doped ZnO were determined using Siemens D5000 X-Ray diffractometer (XRD) with the CuKα (λ=0.15405 nm) radiation. The optical properties of nanoparticles were determined by UV-Vis spectra recorded by a Beckman Coulter DU800 spectrophotometer. FT-IR analyses were performed using digilab FTS 1000 SCIMITAR Series FTIR pectrophotometer. Raman spectra were obtained using

Jobin-Yvon T64000 Raman spectrometer

3 RESULT AND DISCUSSION

3.1 XRD Analyses

Figure 1 shows the XRD patterns of Fe-doped ZnO solids synthesized at different atomic fractions of Fe (x = 0.0-0.1).

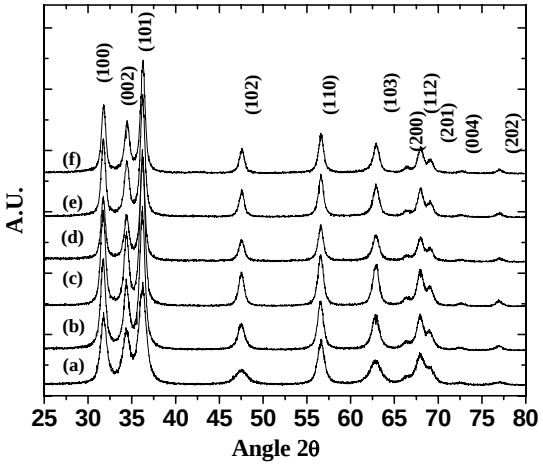

Figure 1: XRD patterns of $Zn_{1-x}Fe_xO$ powders; 'x'= 0.00(a), 0.01(b), 0.03(c), 0.05(d), 0.08(e), 0.1(f).

XRD analyses confirm that the wurtzite structure of ZnO does not change after Fe doping. The absence of any impurity phase (FeO, Fe_2O_3 or $ZnFe_2O_4$), suggests that Fe^{2+} successfully substituted the Zn^{2+} in ZnO lattice.

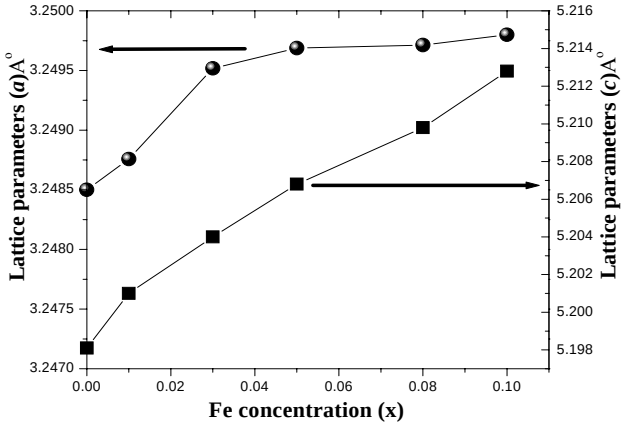

Figure 2: Variation in lattice parameters 'a' and 'c', of host ZnO as a function of the dopant atomic fraction 'x', (x= 0.01-0.10).

Average crystallite size, estimated by Scherrer's equation, ranged from 11 nm to 13 nm when the 'x' value rises from 0.0 up to 0.1. A systematic shift in the position of XRD peaks with 'x' values was also evident from careful analysis of XRD data. These shifts suggest a change in the lattice parameters of host ZnO. Figure 2 shows the variation in 'a' and 'c' parameters in the 'x' range from 0.01 to 0.1. The lattice parameter 'c' increases monotonically from 5.1991 Å, for x=0.0.1 to 5.2106 Å for x =0.10. The corresponding 'a' lattice parameter increases from 3.2485 Å to 3.2498 Å. It may be due to the distortion in host ZnO structure by substitution of Zn^{2+} (ionic radius 0.60 Å) by slightly greater Fe^{2+} (ionic radius 0.63Å).

3.2 FT-IR Measurements

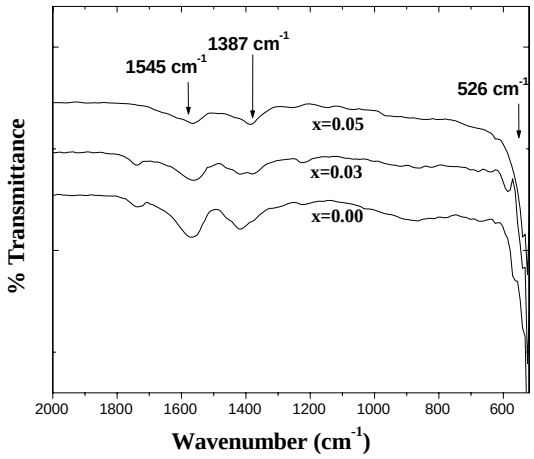

Figure 3: FT-IR spectra of Fe- doped ZnO nanoparticles synthesized at different Fe atomic fraction, 'x'.

The FT-IR spectra of the nanocrystalline Fe-doped ZnO particles synthesized at different 'x' values are shown in Figure 3. The band at 526 cm^{-1} is assigned to the Zn-O or Fe-O stretching vibrations. Moreover, the FT-IR spectra show two broad bands at about 1565 cm^{-1} and 1424 cm^{-1}, which do not change upon increasing the iron concentrations. The band at 1565 cm^{-1} was assigned to the C=C stretching bond while the band at 1424 cm^{-1} appeared due to C=O stretching bond. The presence of these two bands can be attributed to the adsorption of acetate species, from precursor metal salts, onto the oxide surface [5]. The presence of these adsorbed acetate species would provide a net negative surface charge on the nanocrystals, which restricted crystal growth and aggregation due to repulsive electrostatic interactions. Adsorbed acetate species can be removed or decompose with thermal treatment above 200°C.

3.3 Raman Measurements

Figure 4 shows the Raman spectra for $Zn_{1-x}Fe_xO$ (x = 0.03, 0.05, 0.08) powders. All the measurements were carried out at room temperature. As the concentration of Fe increases from 0.03 to 0.08, the ZnO phonon mode shifted

from 433 cm^{-1} to 421 cm^{-1}. It may be due to the decrease in binding energy of Zn-O bond as a result of substitution of Zn^{2+} with Fe^{2+}. The peak at about 668 cm^{-1} is due to the substitution of Fe^{2+}. The intensity of the peak at about 668 cm^{-1} increases with the increase in Fe^{2+} concentration, indicating the incorporation of Fe^{2+} in ZnO.

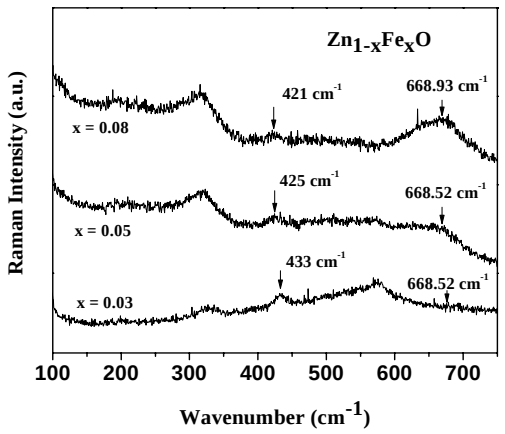

Figure 4: Raman spectra of Fe-doped ZnO nanoparticles with varying atomic fraction of Fe, (x = 0.03-0.08)

3.4 Magnetic Characterization

Room-temperature SQUID measurement suggested the actual incorporation of dopant species into the otherwise diamagnetic ZnO host structure (Figure 5).

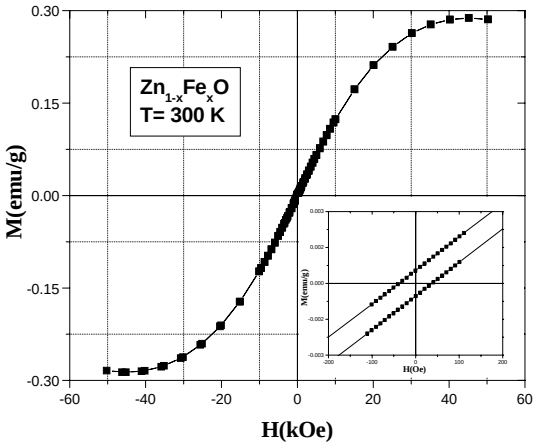

Figure 5: M-H curves for as-synthesized Fe-doped ZnO nanoparticles ('x' = 0.08) at 300K, after subtraction of paramagnetic component.

The Fe-doped ZnO ('x'=0.08) exhibited a weak ferromagnetism at 300 K. The inset is a magnification of the same figure and shows a small, though noticeable, coercivity (46 Oe), which suggests a weak ferromagnetism at room temperature. Despite this apparent ferromagnetism, our current results can not rule out the formation of ferrimagnetic magnetite (Fe3O4) or other secondary phases that could account for the observed magnetic response. Ongoing work is focused on the analysis of this possibility. On the other hand, doped nanoparticles exhibited paramagnetic behavior at higher magnetic fields.

4 CONCLUDING REMARKS

We have successfully synthesized Fe doped ZnO nanoparticles at low temperature and with no need of any thermal treatment of the sample to develop the oxide structure. The lattice parameters of the particles were found to increase on increasing the Fe^{2+} concentration, suggesting actual incorporation of dopant in the ZnO lattice. Raman spectra confirm the incorporation of Fe^{2+} into ZnO lattice. Room-temperature SQUID analyses suggested the actual incorporation of Fe ions into otherwise diamagnetic ZnO structure. Doped nanoparticles synthesized at 'x'=0.08 exhibited a paramagnetic behavior at high magnetic fields, although a small coercivity became evident at lower fields.

5 ACKNOWLEDGMENTS

This material is based upon work supported by the National Science Foundation under Grant No. 0351449. Any opinions, findings and conclusions or recommendations expressed in this material are those of the author(s) and do not necessarily reflect the views of the National Science Foundation (NSF). Thanks are also extended to NSF-Start Up Program for providing partial support for this research. We also appreciate the contribution from Dr. C. Rinaldi with SQUID measurements.

REFERENCES

[1] He. Yong-Ning; Zhu Chang-Chun; Zhang Jing-Wen Microelectronics journal. Vol 35. n° 4. pp. 389-392. 2004.

[2] Kadota, M., Konvo, C., Ikeda, T., and Kasanami.Microelectronics journal T.: Jpn. J. App. Phys., Vol 29, (Suppl. 29-I). pp. 159-161. 1990.

[3] E. M. C. Fortunato, P. M. C. Barquinha, A. C. M. B.G. Pimentel, A. M. F. Gonçalves, A. J. S. Marques, L. M. N. Pereira, R. F. P. Martins. Advanced Materials, Vol 17. pp 590-594. 2005.

[4] Spanhel, L. Anderson, M. A. J. Am. Chem. Soc.Vol 113. pp 2826-2833. 1991.

[5] S.P. Singh, O. Perales-Perez, M.S. Tomar, A. Parra-Palomino and A. Ruiz-Mendoza. Technical Proceedings Nanotechnology Conference, Vol 2. pp 29-32. 2005.

[6] H. Katayama-Yoshida, K Sato / Jpn. J. Appl. Phys B Vol 39. pp L555. 2000.

[7] Dietl, H.Ohno, F. Matsukura, J.Cibert. & D. Ferrand, Science. Vol 287. pp 1019. 2000.
[8] Kwang Joo Kima) and Young Ran Park. Appl. PhysLett. Vol 81. pp 1420-1422. 2002.
[9] Subhash Thota, Titas Dutta and Jitendra Kumar, J.Phys. Condensed Matter, Vol 18. pp. 2473. 2006.